

- [4] E. Donchin, K. Spencer, and R. Wijesinghe. The mental prosthesis: Assessing the speed of a P300-based brain-computer interface. *IEEE Trans. Rehabil. Eng.*, 8(2):174–179, Jun. 2000.
- [5] G. Dornhege, B. Blankertz, G. Curio, and K.-R. Müller. Boosting bit rates in noninvasive EEG single-trial classifications by feature combination and multiclass paradigms. *IEEE Transactions on Biomedical Engineering*, 51(6):993–1002, 2004.
- [6] O. Friman, I. Volosyak, and A. Gräser. Multiple channel detection of steady-state visual evoked potentials for brain-computer interfaces. *IEEE Trans. Biomed. Eng.*, 54(4):742–750, Apr. 2007.
- [7] R. Kus, D. Valbuena, J. Zygierevich, T. Malechka, A. Gräser, and P. Durka. Asynchronous BCI based on motor imagery with automated calibration and neurofeedback training. *IEEE Transactions on Neural Systems and Rehabilitation Engineering*, 1:1–13, 2012.
- [8] J. Müller-Gerking, G. Pfurtscheller, and H. Flyvbjerg. Designing optimal spatial filters for single-trial eeg classification in a movement task. *Clinical neurophysiology*, 110:787–798, 1999.
- [9] C. Neuper and G. Pfurtscheller. Event-related dynamics of cortical rhythms: frequency-specific features and functional correlates. *Int. J. Psychophysiol.*, 43(1):41–58, Dec 2001.
- [10] M. A. Pastor, J. Artieda, J. Arbizu, M. V., and J. C Masdeu. Human cerebral activation during steady-state visual-evoked responses. *J. Neurosci.*, 23(37):11621–11627, Dec. 2003.
- [11] G. Pfurtscheller, B. Z. Allison, C. Brunner, G. Bauernfeind, T. Solis-Escalante, R. Scherer, Th. O. Zander, G. Mueller-Putz, Ch. Neuper, and N. Birbaumer. The hybrid BCI. *Frontiers in Neuroscience*, 2:1–11, 2010.
- [12] G. Pfurtscheller and F. H. Lopes da Silva. Event-related EEG/MEG synchronization and desynchronization: basic principles. *Clinical Neurophysiology*, 110(11):1842–1857, 1999.
- [13] G. Pfurtscheller, T. Solis-Escalante, R. Ortner, and P. Linortner. Self-paced operation of an SSVEP-based orthosis with and without an imagery-based “brain switch”: A feasibility study towards a hybrid BCI. *IEEE Trans. Neural Syst. Rehabil. Eng.*, 18:409–414, Feb. 2010.
- [14] D.T. Pham and J.-F. Cardoso. Blind separation of instantaneous mixtures of nonstationary sources. *IEEE Transactions on Signal Processing*, 49(9):1837–1848, 2001.
- [15] R. Leeb, H. Sagha, R. Chavarriaga, and J. Del R Millan. A hybrid brain-computer interface based on the fusion of electroencephalographic and electromyographic activities. *J Neural Eng*, 8(2):025011, Mar 2011.
- [16] R. Scherer, G. R. Müller-Putz, and G. Pfurtscheller. Self-initiation of eeg-based brain-computer communication using the heart rate response. *J. Neural Eng.*, 4(4):L23–L29, Dec 2007.
- [17] E. W. Sellers, D. J. Krusienski, D. J. McFarland, Th. M. Vaughan, and J. R. Wolpaw. A P300 event-related potential brain-computer interface (BCI): The effects of matrix size and inter stimulus interval on performance. *Biol. Psychol.*, 73:242–252, 2006.
- [18] A. Souloumiac. Nonorthogonal joint diagonalization by combining givens and hyperbolic rotations. *IEEE Trans. Signal Proc.*, 57:2222–2231, 2009.
- [19] R. Vilimek and Th. O. Zander. BC(eye): Combining Eye-Gaze Input with Brain-Computer Interaction. In *Universal Access in HCI, Part II, HCI 2009, LNCS 5615*, pages 593–602. Springer, 2009.
- [20] I. Volosyak, D. Valbuena, T. Lüth, T. Malechka, and A. Gräser. BCI Demographics II: How many (and what kinds of) people can use an SSVEP BCI? *IEEE Trans. Neural Syst. Rehabil. Eng.*, 19(3):232–239, Jun. 2011.
- [21] Y. Wang, R. Wang, X. Gao, B. Hong, and S. Gao. A Practical VEP-Based Brain-Computer Interface. *IEEE Trans. Neural Syst. Rehabil. Eng.*, 14(2):234–239, Jun 2006.
- [22] T.O. Zander, M. Gaertner, C. Kothe, and R. Vilimek. Combining eye gaze input with a brain-computer interface for touchless human-computer interaction. *Int. J. Human-Computer Interaction*, 27(1):38–51, 2011.
- [23] A. Ziehe, P. Laskov, G. Nolte, and K.R. Müller. A fast algorithm for joint diagonalization with non-orthogonal transformations and its application to blind source separation. *Journal of Machine Learning Research*, 5:777–800, 2004.

On the Formulation of Parallel Position/Force Control Schemes for Industrial Manipulators

M. İ. C. DEDE¹, M. K. ÖZGÖREN²

¹İzmir Institute of Technology, Department of Mechanical Engineering, İzmir, Turkey
Email: candede@iyte.edu.tr

²Middle East Technical University, Department of Mechanical Engineering, Ankara, Turkey
Email: ozgoren@metu.edu.tr

Keywords: *position/force control, impedance control, admittance control, hybrid control*

Abstract

In this paper, three commonly-used position/force control schemes namely Impedance, Admittance and Hybrid Position/Force control are investigated for use in industrial manipulators. In order to eliminate the instability problem that may occur in the customary versions of these schemes for large position errors, a modification is proposed, which is based on determining the joint-space position errors using inverse kinematic solutions rather than using the inverse Jacobian matrix. The feasibility of this modification relies on the fact that almost all of the industrial manipulators have easily obtainable inverse kinematic solutions. The simulation results showing the performance of the modified control schemes are also presented as applied on a Puma 560 manipulator.

1. Introduction

These days the robots are required to comply with their environment more often than ever. This calls for new robot architectures with more sensors and control schemes which not only control the positions of the robot manipulators but also the forces exerted by them to the environment. Commonly encountered schemes in the related literature that may be used to control the position and the applied forces and/or moments are the Impedance, Hybrid Position/Force Control and the Admittance Control [1]. However, in these schemes, the position error is formed by comparing the reference input (desired position) and the measured data (actual position) with each other in the Cartesian space. This error is transformed into the joint space as a linear approximation by using the inverse of the Jacobian matrix. The approximate error calculated in the joint space is then fed into the control unit to drive the joint actuators. This method can be used to control the manipulator successfully if the error calculated in the Cartesian space is small. The system behavior deteriorates and it may even become unstable as this error increases. It is a known fact that, the inverse kinematic solutions can be obtained quite easily for many manipulators used in practice [2], [3]. The exact position error for such a manipulator can be evaluated directly in the joint space by first finding the joint space equivalents of the desired and actual positions separately through the inverse kinematics and then comparing them.

Necessary modifications are proposed in this paper to be incorporated into the customary Impedance, Hybrid Position/Force Control and the Admittance Control schemes to evaluate position error directly in the joint space as described above. The modified control schemes are tested in simulation for certain tasks. Simulation results are presented to demonstrate the performance achieved with these modifications.

2. Problem Definition

Restricting one or more of the manipulator's motion along certain directions, while it performs a desired motion, by applying forces in those directions may cause instability [4].

Unlike the simple modification introduced in [5, 6], many of the researchers in this area have so far concentrated generally on making the conventional position/force control schemes more sophisticated by introducing adaptive or learning features [7, 8] in order to cope with this problem. While forming such sophisticated controls, the comparison methods for calculating the position errors of the customary position/force control schemes are kept unmodified. The possible instability due to the customary control schemes is discussed in the MSc thesis of Dede [5]. The instability problem for the customary position/force control schemes arises when there are increases in the errors calculated for the position-controlled subsystem in the Hybrid Position/Force Control scheme and for the position-controlled inner control loop in the Impedance and Admittance Control schemes. This is basically due to the previously mentioned fact that the position errors in the joint space are obtained approximately by the linear transformation of the actual position errors in the Cartesian space through the inverse Jacobian matrix.

3. Customary Position/Force Control Schemes

In this section the customary schemes for position/force controllers are introduced as they are used in the related literature. The first control algorithm discussed is the Impedance Control which is followed by the Admittance and Hybrid Position/Force Control.

3.1 Customary Impedance control

The objective of impedance control is to establish a desired dynamical relationship between the end-effector position and the applied force [9]. The relationship between the velocity \dot{X} and the applied force F is referred to as the mechanical impedance, Z_m . In the s domain, this is represented by

$$F(s) = Z_m(s)\dot{X}(s). \quad (1)$$

Equation (1) is rewritten to relate the position, $X(s)$, to the force by

$$F(s) = sZ_m(s)X(s). \quad (2)$$

Desired impedance is specified as;

$$sZ_m(s) = Ms^2 + Ds + K. \quad (3)$$

The constant matrices M , D and K represents the desired inertia, damping and stiffness values, respectively. Typically, as in this case, the target impedance is chosen as a linear second-order system to mimic mass-spring-damper dynamics [4]. The task of Impedance control is to guarantee the behavior of the controlled system to be as dictated by equation (3). Impedance control has been implemented in various forms, depending on how the measured signals including velocity, position or force are used.

The order of the impedance control depends on how the impedance term is defined. If the impedance term is defined as a spring, then the control scheme is called a zeroth-order Impedance control, which is commonly known as the Stiffness control [10]. Second-order Impedance control that is applied to a position-based control system is shown in Figure 1, in which X_F represents the equivalent force-feedback trajectory, X_I is the modified desired trajectory defined as the solution to the differential equation

$$M\ddot{X}_I + D\dot{X}_I + KX_I = -F + M\ddot{X}_D + D\dot{X}_D + KX_D, \quad (4)$$

where $X_I(0) = X_D(0)$, $\dot{X}_I(0) = \dot{X}_D(0)$. M , D and K are as defined before. Equation (4) can be obtained by inspection from Figure 1. It implies the same impedance definition as in equations (2) and (3). It is noted that in the Impedance control formulation X_I is a function of both the input, X_D , and the measured contact force, F . Since the position-controlled subsystem ensures that the end-effector position X closely tracks X_I defined in equation (4), the target impedance of the manipulator is obtained [11].

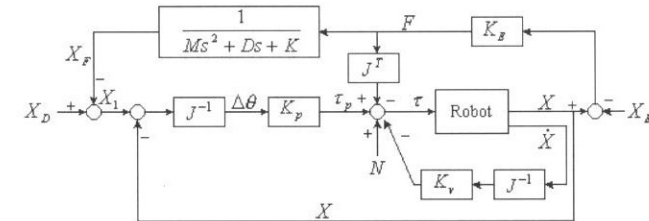


Fig.1. Customary position-based second-order Impedance Control scheme

In Figure 1, and in the following Figures 2, 3, 4, 5 and 6, "N", represents the feed-forward torque input to counteract the centrifugal, Coriolis and gravitational forces [11]. The other feed-forward torque input " $J^T K_E (X - X_E)$ " is generated to counteract the effect of the environmental interaction forces [7]. Here, " K_E " is the combined stiffness matrix of the environment and the force sensors. In this work, however, environment is modeled as rigid, and therefore, " K_E " is associated only with the force sensors.

Sensor-based feedback-controlled interaction with the environment requires the impedance to be of second order at most. The reason for this is that the dynamics of a second-order system are well understood and familiar and for higher-order systems, it is difficult to obtain measurements corresponding to the higher-order state variables [13].

3.2 Customary Admittance control

Admittance control specifies a force setpoint, which is tracked by a force compensator. In contrast with a pure position control, which rejects disturbance forces in order to track a given reference motion trajectory, the force compensator attempts to comply with the environmental interaction and reacts quickly to contact forces by rapidly modifying the reference motion trajectory [14]. The mechanical admittance is defined as

$$\dot{X}(t) = AF(t). \quad (5)$$

This equation can be written in the s domain as

$$X(s) = K(s)F(s), \quad (6)$$

where

$$K(s) = \frac{1}{s}A. \quad (7)$$

In equations (5), (6) and (7), X and \dot{X} are the position and velocity vectors of the end-effector, A is the admittance matrix, and Figure 2 shows the structure of a customary admittance control scheme.

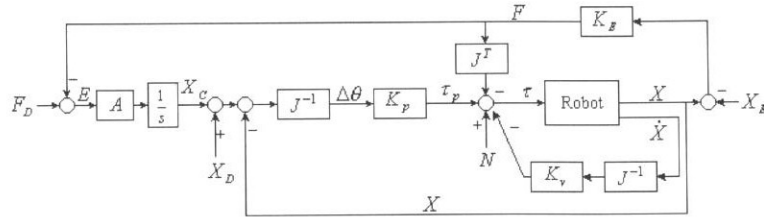


Fig.2. Customary position-based Admittance Control scheme

The admittance matrix, A , in Figure 2, relates the force error vector, E ($E = F_D - F$), to the required modification in the end-effector velocity vector. This leads to the following additive modification on the reference trajectory:

$$X_c = \int A(F_D - F)dt. \quad (8)$$

Admittance control can be effectively and precisely achieved by choosing a suitable A matrix for the known stiffness of the environment. However, if the working environment changes significantly, A matrix should be recalculated in order to adapt the new environment. Changing the admittance value properly due to the changing environment may be realized with adaptive control laws. In general, though, it can be said that the value of the A matrix should decrease as the stiffness of the environment increases causing larger amount of forces to be exerted with the same amount of motion toward the surface. An adaptation to changing environments is also necessary for selecting the impedance term in Impedance control.

Although equations (5)-(8) imply that A is constant, it is also possible, and in fact expedient, to extend the concept of admittance to involve a variable matrix such as

$$A(s) = k_d s^2 + k_p s + k_i, \quad (9)$$

which then results in the following PID force compensator:

$$K(s) = \frac{1}{s} \cdot A(s) = k_d s + k_p + \frac{k_i}{s}. \quad (10)$$

3.3 Customary Hybrid Position/Force control

Combining position and force information into one control scheme for moving the end-effector in nondeterministic environments has been introduced as hybrid position/force control [15]. The advantage of hybrid position/force control with respect to others is that the position and force information are processed independently by separate controllers to take advantage of well-known control techniques for each of them. The outcomes of these controllers are then combined only at the final stage when both have been converted to joint torques [16]. Figure 3 shows the application of the hybrid position/force control scheme as a block diagram.

In Figure 3, $S = \text{diag}(s_j)$ ($j = 1 \dots n$) is called the compliance selection matrix, n represents the degree of freedom. The matrix S determines the subspaces in which force or position are to be controlled, and s_j is selected as either 1 or 0. When $s_j = 0$, force control must be used in the j^{th} direction of the Cartesian space; otherwise, position control must be used in that direction. Depending on the required task, S matrix can be constant, or it can change in time according to the varying gradient of the task surface and the path followed on it [17].

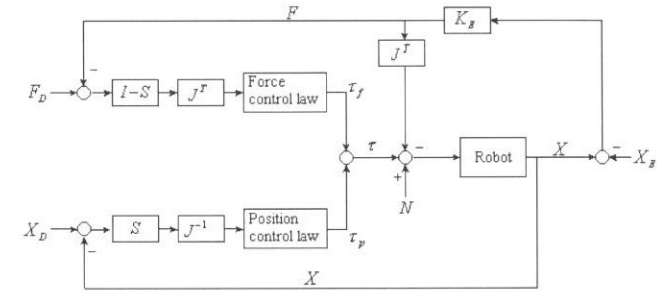


Fig. 3. Customary Hybrid Position/Force Control scheme

For each task configuration, a generalized surface can be defined with position constraints along the normals to this surface and force constraints along the tangents. This means that the end-effector cannot move along the normals into the surface and cannot cause reaction forces to arise along the tangents of the surface. These two types of constraints partition the freedom directions of possible end-effector motions into two orthogonal sets along which either position or force control must be used [14]. Utilizing this partitioning, S matrix is formed appropriately in accordance with the required task.

In this control scheme, the command torque is

$$\tau = \tau_p + \tau_f \quad (11)$$

τ_p and τ_f are the command torques acting in the position and force subspaces, respectively. In this way, position control and force control are decoupled. In general, it happens that PD action is satisfactory for position control, and PI action is satisfactory for force control [1].

4. Modified Position/Force Control Formulations

As pointed out above, for position control, PD action is preferred in both of the Hybrid and Admittance control schemes. However, in the customary versions of these schemes, as seen in Figures 1, 2 and 3, the Cartesian-space position error ($X_{ref} - X$) is assumed to be small and therefore it is transformed into the joint space approximately as

$$(\theta_{ref} - \theta) \approx J^{-1}(X_{ref} - X). \quad (12)$$

It turns out that this approximation often leads to unsatisfactory behaviors if the position error becomes large. As a proposal of remedy, the Impedance, Admittance and Hybrid

Position/Force control schemes are modified here as described below. This modification is based on calculating the joint-space position error exactly as follows:

$$(\theta_{ref} - \theta) = IK(X_{ref}) - IK(X). \quad (13)$$

Here, "IK" symbolizes Inverse Kinematics and this modification is of course feasible for those manipulators for which "IK" solutions are easy to obtain. Fortunately though, almost all of the industrial manipulators are of this kind [2], [3].

4.1 Modified Impedance control

Inner position loop of the Impedance Control scheme is modified to make the necessary comparisons in the joint space and not in the Cartesian space as it was for the customary version. Figure 4 shows the modified version of the Impedance Control scheme.

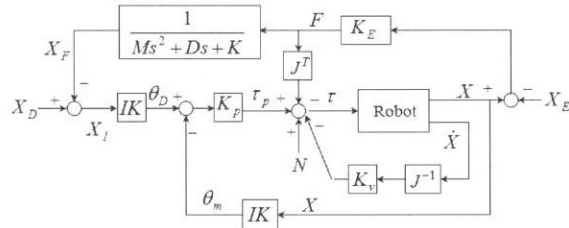


Fig.4. Modified Impedance Control scheme

Position feedback of the end-effector is changed to joint position feedback by inverse kinematics "IK" in the modified scheme. The inverse kinematics solutions can be achieved easily by using the methodology introduced in [2]. Besides, in a real time application, position feedbacks are received directly from the joint transducers. Therefore, it is sufficient to employ inverse kinematics only for the reference position $X_I = X_D - X_F$ defined in the Cartesian space.

4.2 Modified Admittance control

Similar to the Impedance Control modifications, inner position loop of the Admittance Control scheme is modified to make the necessary comparisons in the joint space and not in the Cartesian space. The modified version of the Admittance Control scheme is presented in Figure 5.

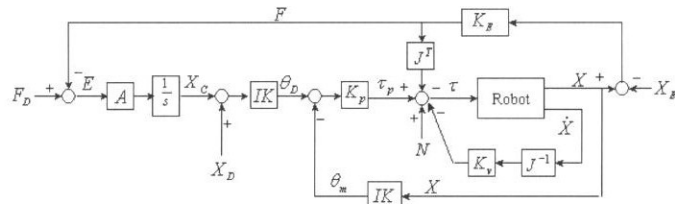


Fig.5. Modified Admittance control scheme

Position feedback of the end-effector is changed to joint position feedback by inverse kinematics "IK" in the modified scheme as it was the case in Impedance Control

modifications. In a real application, it is also sufficient to employ inverse kinematics only for the reference position $X_{ref} = X_C + X_D$ defined in the Cartesian space.

4.2 Modified Hybrid Position/Force control

Hybrid control scheme is also modified to make the necessary comparisons in the joint space and not in the Cartesian space as shown in Figure 6. Again, "IK" in the figure represents Inverse Kinematics.

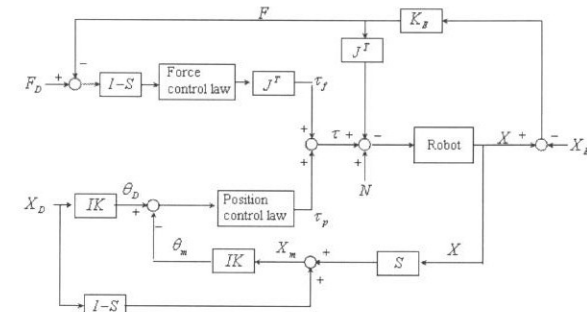


Fig.6. Modified Hybrid Position/Force control scheme

This modified version of the Hybrid Control does not use the selection matrix, "S" after the comparison is made in the Cartesian Space for the position control subspace. The selection matrix is used to take the measured positions along the directions to be position controlled as they are and modify the measured position along the direction to be force controlled to the desired position along that direction. This makes the position error along the direction to be force controlled equal to zero, which means that the controller working in the position control subspace will not try to monitor the position along the force control direction.

After these modifications on the measured position, "X", the modified measured position, "X_m", is transformed to the Joint Space to calculate the modified measured joint angles, "theta_m", using the inverse kinematics equations. Desired position vector is also transformed to the Joint Space using the inverse kinematics equations. As a result of this, the comparison is made in the Joint Space and the outcome is fed into the position controller.

5. Simulation Test Results

The PUMA 560 6R manipulator, for which the system parameters are described in Bascuhadar's thesis [18], is used for numerical simulations. Point type of contact and the force sensor are considered to be at the end point of the end-effector for this study. All the simulations are carried out in Matlab© Simulink environment. The forward kinematics and system dynamics are modeled using the Simmechanics module of Matlab©.

No surface or joint friction is modeled for the simulations presented in this paper for the sake of simplicity. The contact is assumed to occur in such a way that only one degree of freedom is constrained by a flat surface normal to $\bar{u}_1^0(X)$ axis as illustrated in Figure 7.

The task to be accomplished for this simulation study is drawing a circle on a flat and rigid surface. The diameter of the circle to be drawn for the Hybrid Control is 0.3 meters and for the Admittance Control is 0.2 meters. This is an arbitrary selection for the diameters with the

only restriction that the circles remain within the workspace of the manipulator. The link and joint parameters of the Puma 560 used in this work are given in Table 1.

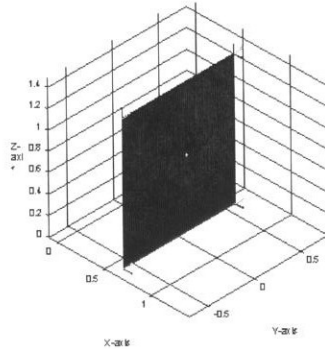


Fig.7. The task plane considered in the simulation examples

The manipulator is required to apply a 15 N pressing force while drawing the circles for the Admittance and Hybrid Controls. However, since the control scheme of Impedance control does not include a force demand input, the Impedance Control scheme tries to reduce the contact forces to zero as smoothly as possible. Figures 8, 9 and 10 show the circle drawn on $\bar{u}_2^0 (Y) - \bar{u}_3^0 (Z)$ plane by the tip of the end-effector when the manipulator is controlled with the modified Impedance, Admittance and Hybrid control schemes, respectively.

Table 1. Link and Joint Parameters of PUMA 560 Manipulator

| Joints | α_k (deg.) | s_k (mm.) | a_k (mm.) | θ_k (deg.) |
|--------|-------------------|-------------|-------------|-------------------|
| 1 - | 90° | 0.0 | | θ_1 |
| 2 0 | | 81.5 | 300 | θ_2 |
| 3 9 | 0° 0 | | 0 | θ_3 |
| 4 - | 90° 30 | 4.5 | 0 | θ_4 |
| 5 9 | 0° 0 | | 0 | θ_5 |
| 6 0 | | 0 | 0 | θ_6 |

$(Ms^2 + Ds + K)^{-1}$ term in Impedance Control is considered as a second order system and the parameters of this term are determined within this assumption. ζ is selected as 0.8 and ω_n is selected as 15, 6 rad/s respectively. Different parameters are tried for the force-controlled outer loop of the Admittance Control and the force-controlled sub-space of the Hybrid Control. Suitable set of parameters lead to the force plots shown in Figures 11, 12 and 13. The corresponding parameters are presented in the legends of these plots. PID control is used for the force-controlled outer loop of the Admittance Control to form the A matrix as in equation (9). PI control is preferred for the force-controlled sub-space of the Hybrid Control.

As for the mobility directions, PD parameters for the position-controlled inner loop of the Impedance Control, Admittance Control and the position-controlled sub-space of the Hybrid Control are selected using the method explained in the thesis of Dede [5], which is also briefly

outlined here: Since the nonlinear feed-forward compensation term “ N ” cancels out the Coriolis, centrifugal and gravitational forces, the reduced equation of motion ($M\ddot{\theta} = \tau^* + \tau'$) resembles to that of a double-integrator plant with control and disturbance inputs τ^* and τ' . Utilizing this fact, the control input is generated with a PD action as

$$\tau^* = K_p(\theta_r - \theta) + K_d(\dot{\theta}_r - \dot{\theta}) \quad (14)$$

and the parameters K_p and K_v are determined as follows:

$$K_v = 2\zeta\omega_n M', \quad (15)$$

$$K_p = \omega_n^2 M'. \quad (16)$$

Here, for sake of simplicity, M' is taken as the diagonal portion of the mass matrix M . The damping ratio ζ is selected as 0.8 and the natural frequency ω_n is selected as 50 rad/s, which happens to be a reasonable value determined after few trials. The position control performance of the manipulator in tracking the required circular paths can also be depicted in Figures 8, 9 and 10 for the Impedance, Admittance and the Hybrid control schemes.

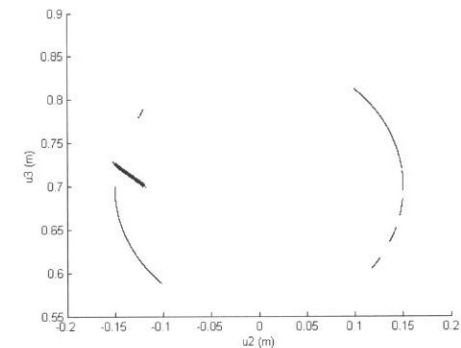


Fig.8. Circle drawn on the task plane by the manipulator using Impedance Control

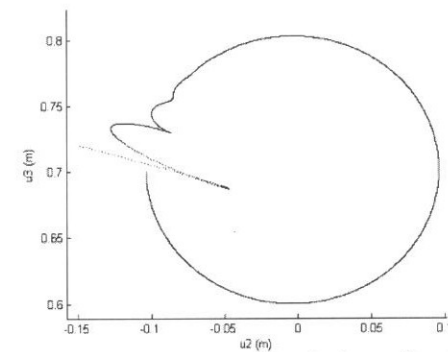


Fig.9. Circle drawn on the task plane by the manipulator using Admittance Control

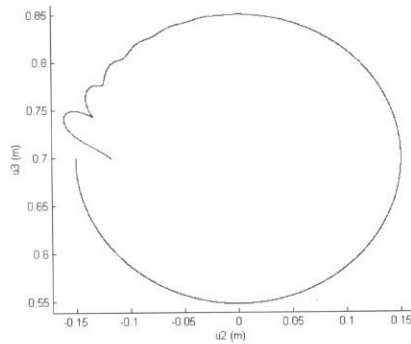


Fig.10. Circle drawn on the task plane by the manipulator using Hybrid Control

It can be clearly seen in Figure 8 that the manipulator is on and off contact with the surface. The line has reduced thickness indicating the decrease in contact forces as a result of the Impedance Control scheme trying to reduce the impact force to zero. As it can be observed from Figures 8, 9 and 10, there are overshoots and oscillations at the beginning of the operation in both control schemes. This is due to the disorientation of the end-effector from the desired one at the beginning and trying to catch up with the desired orientation as the operation continues. The initial overshoots and oscillations can be eliminated to a large extent by starting the operation at the correct orientation or by giving the manipulator some time to correct its orientation before starting the task. Another fact to be pointed out is that the operation does not necessarily start at contact with the surface and it takes varying amount of time for each control scheme to drive the end-effector into contact. Moreover, for the Hybrid Control application, it is required to switch to a pure position controller until the contact is established.

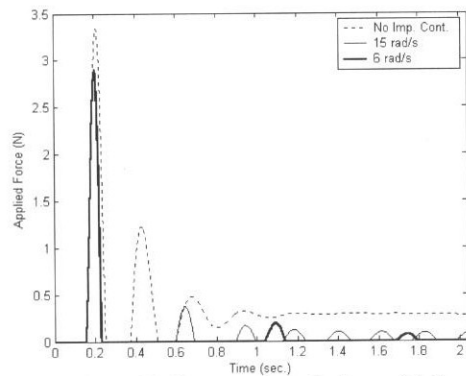


Fig.11. Force applied by the end-effector to the task plane with the modified Impedance Control scheme

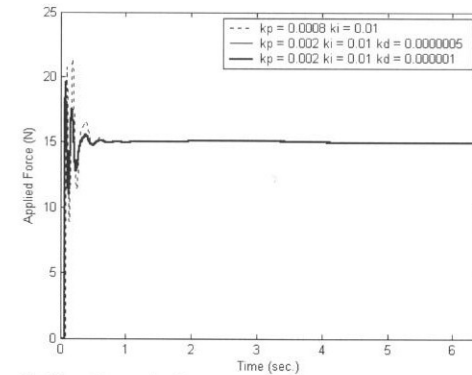


Fig.12. Force applied by the end-effector to the task plane with the modified Admittance Control scheme

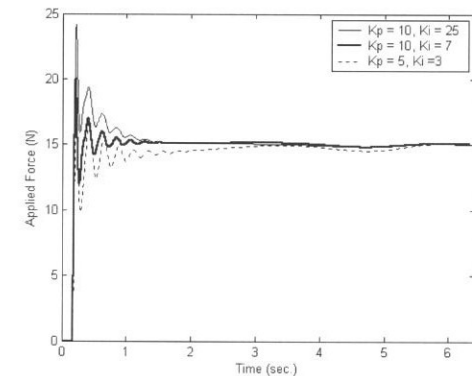


Fig.13. Force applied by the end-effector to the task plane with the modified Hybrid Control scheme

6. Conclusions

In the proposed modifications to the position/force control schemes investigated in this paper, the position errors in the joint space are determined exactly by using the inverse kinematics solution instead of determining them approximately by means of the inverse Jacobian matrix as in the customary schemes. Therefore, it becomes possible with the modified schemes to eliminate the instability problem that may occur in the customary schemes when the initial errors are large or when the end-effector is distracted largely from its desired course by a heavy disturbance. One source of disturbance can be the communication delays or losses that teleoperation systems may experience. In fact, these types of position/force controllers are widely used as teleoperation subsystem controllers.

The overshoots and oscillations that are observed in the simulations during the transient phase of both control schemes may be reduced, even if the starting orientation of the end-effector is not as desired, by using more elaborately determined control gains that contain scheduling with error and/or time. Such an improvement can be studied as an extension of this work. Other items that may be considered in an extended study include surfaces other than

planar ones, edge and surface contacts in addition to point contacts, and contacts with friction involving stick/slip motions.

- [1] G. Zeng and A. Hemami: An Overview of Robot Force Control, *Robotica*, Vol. 15, 1997, pp. 473 - 482.
- [2] M. K. Özgören: Topological Analysis of 6-Joint Serial Manipulators and Their Inverse Kinematics Solutions, *Mechanism and Machine Theory*, Vol. 37, 2002, pp. 551 - 547.
- [3] T. Balkan, M. K. Özgören, M. A. S. Arkan, H. M. Baykurt: A Kinematic Structure-Based Classification and Compact Kinematic Equations For Six-DOF Industrial Robotic Manipulators, *Mechanism and Machine Theory*, Vol. 36, 2001, pp. 817 - 832.
- [4] Q. P. Ha, H. Q. Nquyen, D. C. Rye and H. F. Durrant-Whyte: Robust Impedance Control of Excavator Dynamics, Australian Centre for Field Robotics, Department of Mechanical & Mechatronic Engineering, The University of Sydney.
- [5] M. I. C. Dede: Position/Force Control of Robot Manipulators, Master's Thesis, Department of Mechanical Engineering, METU, Ankara, 2003.
- [6] M. I. C. Dede, and M. K. Özgören: A New Approach for the Formulation of the Admittance and Hybrid Position/Force Control Schemes for Industrial Manipulators, *Proceedings of the 10th Robotics & Remote Systems Mtg. Proceedings*, pp. 332 - 337, Gainesville, Florida, March 28-31, 2004.
- [7] C. J. Tsaprounis and N. A. Aspragathos: Sliding Mode with Adaptive Estimation Force Control of Robot Manipulators Interacting With An Unknown Passive Environment, *Robotica*, Vol. 17, 1999, pp. 447 - 458.
- [8] N. Saadia, Y. Amirat, J. Pontnau and N. K. M'Sirdi: Neural Hybrid Control of Manipulators, *Stability Analysis, Robotica*, Vol. 19, 2001, pp. 41 - 51.
- [9] N. Hogan: Impedance Control: Approach to Manipulation: Part I-Theory, *Journal of Dynamic Systems, Measurements, and Control*, Vol. 107, March 1985, pp. 1 - 7.
- [10] M. Vukobratovic and D. Stokic, 1989: *Applied Control of Manipulation Robots*, Springer-Verlag, Berlin, pp. 353 - 358.
- [11] M. Pelletier and M. Doyon, 1994: On the Implementation and Performance of Impedance Control on Position Controlled Robots, *IEEE Int. Conf. On Robotics and Automation*, pp. 1228 - 1233.
- [12] K. S. Fu, R. C. Gonzalez and C. S. G. Lee: *Robotics: Control, Sensing, Vision, and Intelligence*, McGraw-Hill Book Co., Singapore, 1987.
- [13] R. Volpe and P. Khosla: The Equivalence of Second Order Impedance Control and Proportional Gain Explicit Force Control: Theory and Experiments, *Experimental Robotics II*, 1993, pp. 3 - 24.
- [14] H. Seraji: Adaptive Admittance Control: An Approach to Explicit Force Control in Compliant Motion, *IEEE Int. Conf. On Robotics and Automation*, 1994, pp. 2705 - 2712.
- [15] M. H. Raibert and J. J. Craig: Hybrid Position/Force Control of Manipulators, *ASME Journal of Dynamic Systems, Measurements, and Control*, Vol. 102, 1981, pp. 126 - 133.
- [16] W. D. Fisher and M. S. Mutjaba: Hybrid Position/force Control: A Correct Formulation, Hewlett-Packard Company, 1991.
- [17] G. Fodor and G. Tevesz: Hybrid Position and Force Control Algorithm Expansion of a Robot Control System, *Periodica Polytechnica Ser. El. Eng.*, Vol. 43, No. 4, 1999, pp. 251-261.
- [18] I. Bascuhadar: Design and Construction of a Robotic Manipulator with Six Revolute Joints, Master's Thesis, Department of Mechanical Engineering, METU, Ankara, 1989.

Functional Safety Assessment for the Assistive Robot FRIEND¹

Leila Fotoohi

Institute of Automation, University of Bremen,
Otto-Hahn-Allee NW1, D-28359 Bremen, Germany

E-Mail: fotoohi@iat.uni-bremen.de, <http://www.iat.uni-bremen.de>

Keywords: *safety analysis, hazard identification, HAZOP, FMEA, FTA, safety monitoring*

Abstract

This paper proposes methods for the safe development of the assistive robot FRIEND. The approach started by the hazard identification via the well known system engineering methods. These methods have been used in avionics and nuclear power plants, and can be applied to the safety critical service robots as well; they reveal all potential hazards at the system and component level during design stages. In this context, the systematic bottom-up (Hazard and Operability Study: HAZOP, Failure mode and Effect Analysis: FMEA) and top-down (Fault Tree Analysis: FTA) hazard identification methods are used to determine safety requirements. For this purpose the software tool APIS IQ-RM Pro² (hereafter referred to as APIS) is used to systematically document the results, also to facilitate version control inside the development group. The tool supports both the FMEA and FTA by a systematic stepwise procedure. The result of hazard identification leads to the safety requirements that determine the safety functions needed to mitigate potential critical hazards in the system.

1. Introduction

Up until now, most service robot development has concentrated primarily on the realization of an operating system with less attention given to safety issues. In the past, some researches have been done in safe development of robot components. The development of light weight robot arms with reduced impact upon contact is a good example in this field as discussed in [1] and [5]. The improvement has been done on mechanical parts using smooth and non-sharp structures. Control strategies have also been modified to reduce inertia and contact impact. However, service robots are often used in a wide range of applications and therefore building an overall safe service robot system is not only achieved by reducing impact upon contact with the user. The safety measurements are system related and depend on the operating tasks. A robot arm, equipped with tactile sensors for impact reduction, might still be unsafe. For example consider a servant robot, if the reaction to the over speed movement of the arm is too slow, or if a fast reaction were to cause a heavy object to slip from the robots hand, the robot would not be safe. Therefore the functional safety is very important and must be considered during the design process. However, the researches on functional and overall safety of the service robot systems are still rare. Here to assure coverage for all hazards in complex service robot like FRIEND, both systematic bottom-up and top-down hazard analysis methods is carried out. The systematic bottom-up hazard analysis provides answers to the question "What consequences does a given hazard

¹ FRIEND is an assistive service robot under development at IAT institute, university of Bremen, more details are given in [2,4]

² APIS IQ-RM Pro is a commercial tool for hazard identification and is available free for education purposes [2].